Self-Monitored Clutter Rate Estimation for the Labeled Multi-Bernoulli Filter

Alexander Scheible, Thomas Griebel, and Michael Buchholz
Institute of Measurement, Control and Microtechnology
Ulm University, Germany
{alexander.scheible, thomas.griebel, michael.buchholz}@uni-ulm.de

***Abstract*—Decision making in automated vehicles is based on the environment model, which is typically computed by a tracking module from information gathered by sensors. Thus, for safe and robust operation of the vehicle, the assessment of the current quality of the tracking module is crucial. This work makes a step towards this goal by providing a clutter rate estimation method with a self-monitored quality assessment for the labeled multi-Bernoulli filter. The significance of the proposed quality index is demonstrated by comparing it with the actual estimation error calculated with ground truth data. The simulation results show that the developed quality index is a meaningful value that can be computed online without the need for ground truth data. Moreover, it is competitive and closely related to the estimation error.**

I. Introduction

In the context of automated driving, the self-monitoring of functional modules is not only a critical feature for safe operation but will also make other advanced features possible. This includes, e.g., an adaptive system where the modules are selected based on context information or the dynamic configuration based on performance requirements [1]. The environmental model is especially important since planning and decision-making depend on it. Furthermore, the continuous monitoring of the intended functionality can be mandatory, e.g., by law in Germany [2].

For the tracking module, the self-assessment aims to provide an estimation of the current tracking performance with regard to some tracking evaluation metrics. This assessment must happen online, meaning no ground truth information is available for this task. Therefore, the usual tracking metrics, e.g., optimal subpattern assignment (OSPA) [3], OSPA2 [4], or generalized OSPA (GOSPA) [5], are not applicable since they all require ground truth information. In addition, Dunik et al. [6] introduced an approach to estimating the tracking reliability through the concept of the reliability index. The proposed reliability index is defined with the concept of an ideal Bayesian filter that provides a ground truth tracking result with no assumptions, approximations, or modeling errors made. Therefore, if it can be determined at all, this theoretical index is also not available online. The difference between the ideal filter result and that of the assessed filter reflects the amount of epistemic uncertainty. The assessed filter introduces this uncertainty through a lack of knowledge, i.e., unknown systematic effects or approximations.

Following their approach of the reliability index, we propose to consider the following points in order to realize an online self-assessment system for the tracking module that is applicable in practice and available online. The first two points build on each other, while the last two can be treated independently of the others.

1) *Assessment of the tracking parameters:* This checks whether the specific parametrization of the tracking algorithm fits the data. This includes, e.g., the process and measurement noise parameters.
2) *Sensitivity of the tracking parameters:* A parameter mismatch worsens the tracking result. Here, the influence of a parameter mismatch on some ground truth tracking evaluation metric is determined. Together with the first point, this makes it possible to estimate the impact of a parameter misconfiguration.
3) *Assessment of the filter design:* Every filter is based on some assumptions. For example, the Kalman filter is only optimal under certain conditions, e.g., linear models and Gaussian distributed noise parameters. This point evaluates whether these assumptions fit the data and how they affect performance.
4) *Assessment of the tracking scenario:* Not every scenario is equally difficult, e.g., many tracks close to each other are more difficult to estimate than a single track. This means that the situation in which the filter operates must be taken into account. Although this point is not included in the reliability index of [6] and can not be influenced, it is assumed to have a significant impact on the absolute performance of the filter.

This paper contributes to the first point of the proposed assessment system, the *assessment of the tracking parameters*. One important parameter is the clutter rate which models the number of measurements not originating from the actual objects. For this, we propose a novel clutter rate estimation for the labeled multi-Bernoulli (LMB) filter [7]. The method includes a self-assessment that provides a quality index (QI). The QI indicates the current quality of the estimation and is, therefore,

Parts of this research have been conducted as part of the PoDIUM project and other parts as part of the EVENTS project, which are both funded by the European Union under grant agreement No 101069547 and No 101069614, respectively. Views and opinions expressed are, however, those of the authors only and do not necessarily reflect those of the European Union or European Commission. Neither the European Union nor the granting authority can be held responsible for them.

a helpful value when the tracking parameters and their influence on the performance are assessed during the second proposed point. Note that we do not perform the sensitivity analysis in this work. The proposed method provides more information than a clutter rate estimation without QI. For example, we will show that the QI can be used to detect situations where the number of clutter does not follow the distribution assumed by the filter, which is not possible without it. The estimation can correctly follow a jumping or drifting time-varying clutter rate. Since we see this work in the larger context of the outlined self-assessment aspects for the tracking module, we do not feed the estimation back into the filter and make adjustments but keep it independent of the tracking parameter.

Summarizing our contributions, we

- propose a novel clutter rate estimation with included self-monitoring that provides a QI, and
- show that the QI is closely related to the estimation error and is, thus, meaningful online information.

II. Related Work

The normalized innovation squared (NIS) [8] is the classical online consistency measure for the Kalman filter. It monitors whether the process and measurement noise are consistent with the incoming measurements. Related to this, there exists the generalized NIS (GNIS) and its version for multi-object tracking, the multi-target GNIS (MGNIS) developed by Mahler [9]. These so-called divergence detectors are methods to test the filter assumptions for consistency. What all three methods have in common is that they consider all assumptions together and do not allow the evaluation of a single parameter. This is a major disadvantage in our context, as it is not possible to differentiate the effects on filter performance per parameter.

A more unified assessment approach, including a component analysis of the filter assumptions, is developed by Griebel et al. in [10], [11]. They proposed a self-assessment method based on subjective logic (SL) for the Kalman filter [10]. Note that SL is an extension of probabilistic logic that is based on subjective opinions [12]. This work was extended in [11] for single-object tracking in clutter with the nearest neighbor association. For this task, methods for the assessment of the detection and clutter rate have been developed. Their clutter rate assessment considers three confidence intervals, namely, 50% confidence around the mean of the expected number of clutter and with 25% below and above the first interval [11]. Then, each interval's theoretical expected number of clutter is compared against the actual data to determine whether the rate fits. Similar to our method, the uncertainty value of SL expresses the statistical uncertainty and indicates the estimation quality. However, the modeling with SL has two main disadvantages in this context. First, it allows only a rough clutter rate estimation because of the discretization. Second, the ordering information is ignored by grouping the number of clutter into categorical intervals. This is needed because SL opinions are mathematically based on Dirichlet distributions which imply categorical distributed data. This is not ideal for clutter estimation, since the number of clutter measurements is naturally ordered. Modeling with SL discards this order.

In this work, we enhance [11] in two main points. First, we extend the method for multi-object tracking with the LMB filter. Second, we overcome the limitations of SL while retaining its explicit notation of uncertainty.

III. Foundations

This section briefly summarizes the main fundamentals of the LMB filter and clutter rate modeling with conjugate priors. We refer to [7], [13] for more details about the LMB filter and to [14] for more details about conjugate priors.

A. Labeled Multi-Bernoulli Filter

The LMB filter [7] is a multi-object tracking algorithm based on finite set statistics (FISST) [15]. It is a real-time capable approximation of the GLMB filter, where the updated GLMB density is replaced by a LMB density [7]. The filter has two steps: prediction and update. Because the prediction step is not essential for the clutter rate estimation, we mainly focus on the update step. For the update, the predicted LMB density is converted to a GLMB density, which can be updated analytically with the formulas given in [13]. Then, the updated GLMB is approximated by an LMB density that matches its first statistical moment [7].

In more detail: If the predicted LMB density is given by the parameters $\{r_+^{(l)}, p_+^{(l)}\}_{l\in\mathbb{L}_+}$, then the updated GLMB density is given by [13]

$$\pi(X|Z) = \Delta(X) \sum_{(I,\theta)\in\mathcal{F}(\mathbb{L}_+)\times\Theta} w^{(I,\theta)}(Z)\, \delta_I(\mathcal{L}(X)) \left[p^\theta(\cdot|Z)\right]^X. \quad (1)$$

Here, $X \in \mathcal{F}(\mathbb{X}\times\mathbb{L}_+)$ is the set of all tracks, where one track is given by its kinematic part $x \in \mathbb{X}$ and its label $l \in \mathbb{L}_+$. $\mathbb{X}$ and $\mathbb{Z}$ are the state and measurement space, $\mathcal{F}(A)$ is the set of all finite subsets of a set A, $Z \in \mathcal{F}(\mathbb{Z})$ is the multi-object measurement, Θ is the space of all valid measurement-to-track associations θ, δ is the generalized Kronecker delta with $\delta_Y(X) = 1$ if $Y = X$ and $\delta_Y(X) = 0$ otherwise, and $w^{(I,\theta)}(Z)$ is the weight of the hypothesis (I,θ).

Following [13], we interpret the weight of a hypothesis as its probability, i.e., if we abbreviate $H := (I,\theta)$, then $P(H \mid Z) = w^H(Z)$. Note that each hypothesis H has a clear measurement-to-track association given by the corresponding θ. For completeness, the equations for w^H and p^θ are given by [13]

$$w^{(I,\theta)}(Z) \propto [r_+]^I \left[1-r_+\right]^{\mathbb{L}_+\setminus I} \left[\eta_Z^\theta\right]^I \quad (2a)$$

$$p^\theta(x,l|Z) = \frac{p_+(x,l)\psi_Z(x,l,\theta)}{\eta_Z^\theta(l)} \quad (2b)$$

$$\eta_Z^\theta(l) = \langle p_+(\cdot,l), \psi_Z(\cdot,l,\theta)\rangle \quad (2c)$$

$$\psi_Z(x,l,\theta) = \begin{cases} \frac{p_D(x,l)g(Z_{\theta(l)}|x,l)}{\kappa(Z_{\theta(l)})} & \theta(l) > 0 \\ 1-p_D(x,l) & \theta(l) = 0, \end{cases} \quad (2d)$$

where $p_+(\cdot,l)$ is the predicated state density of label l, r_+ is the predicted existence probability, p_D is the detection probability,

g is the measurement model, $\langle \cdot, \cdot \rangle$ denotes the scalar product in L_2 and κ is the clutter intensity, i.e., the clutter rate per volume. In Eq. (2a) the notation $[f]^A$, where f is a value that depends on $a \in A$ and A is a set, is defined as $[f]^A := \prod_{a \in A} f(a)$.

The LMB density that matches the first moment of Eq. (1) is given by the parameters $\{r^{(l)}, p^{(l)}\}_{l \in \mathbb{L}_+}$ with [7]

$$r^{(l)} = \sum_{\substack{(I,\theta) \in \mathcal{H} \\ l \in I}} w^{(I,\theta)}(Z), \tag{3a}$$

$$p^{(l)} = \frac{1}{r^{(l)}} \sum_{\substack{(I,\theta) \in \mathcal{H} \\ l \in I}} w^{(I,\theta)}(Z) p^{\theta}(x, l|Z), \tag{3b}$$

where $\mathcal{H} := \mathcal{F}(\mathbb{L}_+) \times \Theta$ is the set of all possible hypotheses.

B. Clutter Model

Within the LMB filter, the clutter measurements are assumed to be independent of the object measurements and follow a Poisson process, i.e., if we denote the clutter measurements by $C \subseteq Z$ and the number of clutter by $\mathcal{C} := |C|$, then $\pi(C) = e^{-\langle \kappa, 1 \rangle} \kappa^C$ and $\mathcal{C} \sim \text{Poi}(\langle \kappa, 1 \rangle)$ [15]. The clutter measurements are independent and identically distributed according to the probability density function (pdf) $\kappa / \langle \kappa, 1 \rangle$. Here, we additionally assume a homogeneous Poisson process, where κ is constant over the measurement space [15]. This means the clutter measurements are completely specified by the clutter rate $\lambda := \langle \kappa, 1 \rangle$.

The clutter rate influences the filter through Eq. (2d), which roughly weights the probability of receiving an object measurement against that of receiving a clutter measurement.

We model our current knowledge about the clutter rate by a Gamma distribution, i.e., $\lambda \sim \Gamma(\alpha, \beta)$, where $\Gamma(\alpha, \beta)$ is the Gamma distribution characterized by the shape $\alpha > 0$ and rate $\beta > 0$. Its pdf is given by [14]

$$f_{\alpha,\beta}(x) = \begin{cases} \frac{x^{\alpha-1} e^{-\beta x} \beta^{\alpha}}{\Gamma(\alpha)} & x > 0 \\ 0 & \text{otherwise.} \end{cases} \tag{4}$$

Here, $\Gamma(\cdot)$ denotes the Gamma function. The mean μ and variance σ^2 of the distribution are given by

$$\mu = \frac{\alpha}{\beta}, \quad \sigma^2 = \frac{\alpha}{\beta^2}. \tag{5}$$

In total, this yields the following clutter model:

$$\mathcal{C} \sim \text{Poi}(\lambda), \tag{6a}$$

$$\lambda \sim \Gamma(\alpha, \beta). \tag{6b}$$

Since the Gamma distribution is conjugate to the Poisson distribution, the posterior of Eq. (6b) given $k \in \mathbb{N}_0$ clutter measurements is also Gamma distributed with [14]

$$[\lambda | \mathcal{C} = k] \sim \Gamma(\alpha + k, \beta + 1). \tag{7}$$

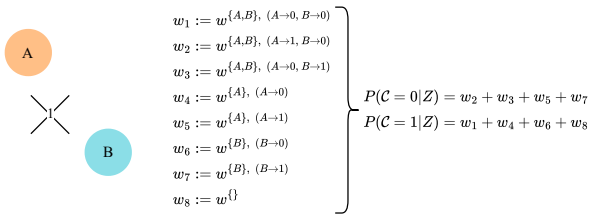

Fig. 1: Illustration of the distribution of the number of clutter. Here, two tracks, indicated by the circles, are updated with one measurement, indicated by the cross. The weights of the updated GLMB hypotheses, cf. Eq. (2), are shown on the middle, with the corresponding clutter distribution on the right, cf. Eq. (8). The association of a track A to a measurement i is denoted $A \to i$, where measurement 0 expresses a misdetection.

IV. Clutter Rate Estimation

We use the Poisson-Gamma model described in Section III-B to express our knowledge about the clutter rate. The mean of the Gamma distribution is the estimation of the clutter rate, whereas the variance is defined as the QI for that estimation and expresses the uncertainty. This means a small QI indicates a confident estimation, and a high QI relates to an unconfident estimation.

To update the clutter estimation, we use the information from the filter update step: A GLMB hypothesis describes one possible association between the tracks and received measurements. The number of clutter in this hypothesis is the number of all non-associated measurements. Using the interpretation of the weight of a hypothesis as its probability according to [13], we compute the distribution of the number of clutter, as illustrated in Fig. 1. With the obtained distribution, we then update the current clutter model. In the following, the method is formulated for the LMB filter. However, it is straightforward to adapt it to other trackers as long as they have an update step that allows the computation of the distribution of the number of clutter, cf. Eq. (8), such as the GLMB filter.

In more detail: Let $N(H) \leq |Z|$ be the number of non-associated measurements of hypothesis H. Then,

$$c_k := P(\mathcal{C} = k|Z) = \sum_{H \in \mathcal{H}} P(\mathcal{C} = k|H) P(H|Z) \tag{8a}$$

$$= \sum_{\substack{H \in \mathcal{H} \\ N(H) = k}} w^H(Z) \tag{8b}$$

is the probability for k clutter measurements.

Using Eq. (8) and Eq. (7), the update of the predicted clutter estimation $\lambda_+ \sim \Gamma(\alpha_+, \beta_+)$ is a mixture of Gamma distributions given by

$$f(\lambda|Z) = \sum_{k \in \mathbb{N}_0} f(\lambda|\mathcal{C} = k) P(\mathcal{C} = k|Z) \tag{9a}$$

$$= \sum_{k \in \mathbb{N}_0} c_k f_{\alpha_+ + k, \beta_+ + 1}(\lambda), \tag{9b}$$

where $f_{\alpha,\beta}$ is the pdf of the Gamma distribution with parameters α, β, cf. Eq. (4).

Note that the sum is actually finite since only a finite number of weights have non-zero values. Moreover, it is worth noting that the computation does not introduce large overhead, as all necessary values are computed by the LMB filter anyway. In theory, the method is analytically closed, as shown above, but the number of mixture components grows rapidly. Therefore, a merging strategy is introduced in the following.

We found that approximating the mixture Eq. (9) by a single Gamma distribution with the same mean and variance as the mixture yields satisfying results for our use case. In detail, let the mixture be given by individual components $i \in \{1, 2, \dots N_C\}$ with mean μ_i, variance σ_i^2, and weight w_i. Then, using the linearity of the expectation and the law of total variance, the mean $\bar{\mu}$ and variance $\bar{\sigma}^2$ of the mixture is given by

$$\bar{\mu} = \sum_{i=1}^{N_C} w_i \mu_i, \tag{10a}$$

$$\bar{\sigma}^2 = \sum_{i=1}^{N_C} w_i \left[\sigma_i^2 + (\mu_i - \bar{\mu})^2\right]. \tag{10b}$$

The Gamma distribution with the same mean and variance, cf. Eq. (5), is given by the parameters

$$\alpha = \frac{\bar{\mu}^2}{\bar{\sigma}^2}, \quad \beta = \frac{\bar{\mu}}{\bar{\sigma}^2}. \tag{11}$$

Because of the association uncertainty expressed in the distribution of $\mathcal{C}$, the variance of the mixture typically will not go to zero. However, it can still become so small that changes and jumps in the clutter rate can be difficult to follow, because of an over-confident predicted estimation λ_+ in Eq. (9). Therefore, we apply two additional steps:

- First, we also include the predicted estimation into the mixture with a fixed weight of $w_{\text{prior}} \in \mathbb{R}_+$, such that Eq. (9) gets replaced by

$$f(\lambda|Z) = w^*_{\text{prior}}\, f_{\alpha_+,\beta_+} + \sum_{k\in\mathbb{N}_0} c^*_k\, f_{\alpha_+ + k, \beta_+ + 1}(\lambda), \tag{12}$$

  where the superscript $*$ denotes that values are normalized, i.e., $w^*_{\text{prior}} + \sum_{k\in\mathbb{N}_0} c^*_k = 1$. This mainly improves the results for rapidly changing or jumping clutter rates. During these periods, there is a discrepancy between the predicted and updated estimation, and this discrepancy will increase the variance of the mixture Eq. (12).
- Second, we apply a discounting step in the prediction by scaling the parameters α, β of the previous estimation by a factor $\varsigma \in (0, 1]$, i.e.,

$$\alpha_+ = \varsigma\alpha, \quad \beta_+ = \varsigma\beta. \tag{13}$$

  This maintains the mean but increases the predicted variance $\sigma^2_+ = \frac{1}{\varsigma}\sigma^2$, cf. Eq. (5). Especially for slowly and smoothly changing clutter rates, where the first step does not help much, this improves the results because it prevents the estimation from becoming overly confident.

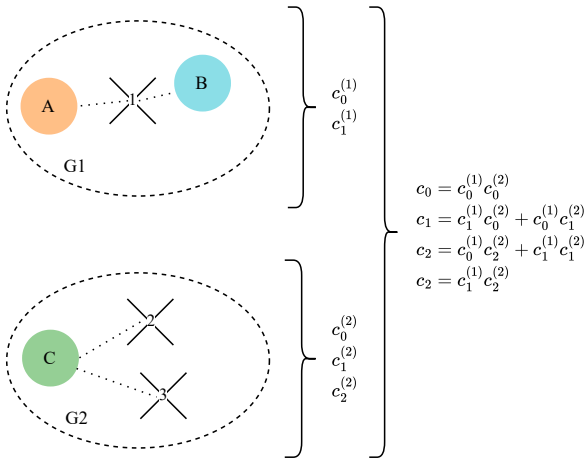

Fig. 2: Illustration of the distribution of the number of clutter when applying grouping in the update step. Here, we have two groups, $G1$ and $G2$, where a non-gated measurement-to-track association is indicated by a dotted line. First, the distribution of each group is calculated as shown in Fig. 1 and Eq. (8). Then, the overall distribution is calculated by considering all possibilities.

V. Handling of Grouping

The key element for the practical applicability of the LMB filter is the gating and grouping step [7]. This breaks the update step into $n \in \mathbb{N}$ independent sub-problems that can be processed in parallel. This is highly advantageous for the filtering, but complicates the computation of the distribution of the number of clutter.

With grouping, every group independently yields the clutter distribution of its sub-problem, as shown in Fig. 2. Then, the overall distribution is given by

$$c_k = \sum_{\substack{k_1+k_2+\dots+k_n=k \\ k_i\in\mathbb{N}_0,\ \forall i=1,\dots,n}} c^{(1)}_{k_1} c^{(2)}_{k_2} \cdots c^{(n)}_{k_n}, \tag{14}$$

where $c^{(i)}$ describes the clutter distribution of group i according to Eq. (8). To compute this efficiently, first, the individual $c^{(i)}$ with non-zero weights are determined. Then, based on the problem size, the sum can either be calculated exactly or approximately by, e.g., a k-shortest path or a sampling-based approach that determines the c_k with relevant weight, such as in [16]. Note that this step does introduce computational overhead.

VI. Experiments and Results

In this section, we perform experiments based on simulated data to test our proposed method. The LMB filter is implemented with Gaussian mixtures based on [7]. We use a simple point measurement model, which measures the (x, y)-position together with a nearly constant velocity state model and a static birth model. The tracking scenario shown in Fig. 3 is simulated with the software in the loop framework [17] and evaluated with 50 Monte-Carlo runs.

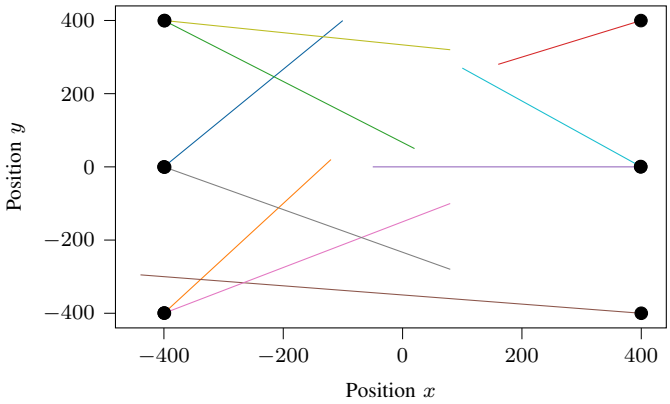

Fig. 3: The simulated tracking scenario with ten tracks. Black circles indicate the start position and the static birth locations.

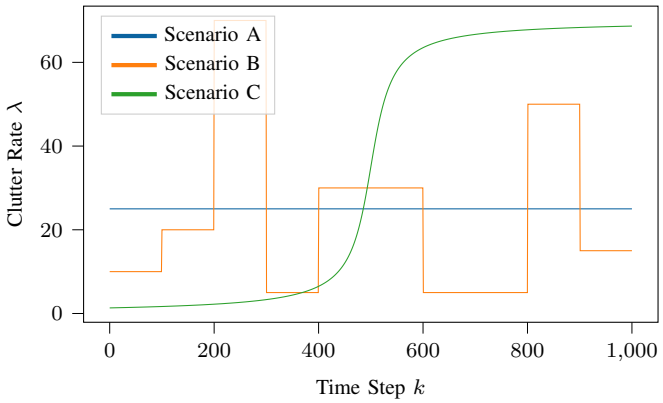

Fig. 4: Three different scenarios with varying clutter rates and profiles.

A. Clutter Profiles

We simulate the tracking scenario with different clutter profiles, where the number of clutter is Poisson distributed with the rates specified in Fig. 4.

In scenario A, the clutter rate is constant but is initialized incorrectly. Scenario B models a clutter rate that jumps between constant values, and scenario C shows a smoothly changing clutter rate. Additionally, we evaluate scenario D, not visualized, where the number of clutter measurements does not follow a Poisson distribution but is uniformly distributed between 0 and 50, i.e., $P(\mathcal{C} = k) = \frac{1}{51},\ k \in \{0, 1, \ldots, 50\}$. In all scenarios, we use the Gamma distribution with mean $\mu = 1$ and variance $\sigma^2 = 10$ as prior for the clutter rate estimation. The prior weight is set to $w_{\text{prior}} = 1$ and the discounting parameter to $\varsigma = 0.95$. The LMB filter assumes a time-invariant clutter rate of 25.

B. Results

Figure 5a and Fig. 5b summarize the results for scenario A. The left figure shows the current estimation of the clutter rate together with the low and high 1% quantile of the estimated Gamma distribution, indicating the uncertainty of the estimation. As expected, the uncertainty drops in the beginning with an increasing number of time steps. However, note that the uncertainty does not decrease significantly because of the association uncertainty inherent to the problem and because of the proposed discount factor. In Fig. 5b, we assess our proposed QI defined by the variance of the estimated Gamma distribution. For this, we compare the QI with the absolute error of the clutter rate estimation. As can be seen, there is a high correlation between the two values, indicating the QI is, in fact, a meaningful value. Note that the QI can be computed online and does not require ground truth information, whereas the estimation error is an offline value that does need ground truth. However, a quantitative evaluation of the QI and its relation to the estimation error, is outside this paper's scope and will be left to future work.

Figure 5c shows the estimation result for the scenario B. Unlike the first scenario, the uncertainty does not drop monotonously but rises at the jumping points of the clutter rate. This is consistent with the error and QI in Fig. 5d. After the jumping times, the uncertainty and error of the estimation drop again. Therefore, also in scenario B, the QI is a strong indicator of the quality of the estimation.

Figure 5e shows the result for the scenario with the continuously drifting clutter rate. Again, according to Fig. 5f, there is a connection between the estimation error and the QI. The larger uncertainty and absolute error after the drift can be explained by the higher ground truth value, so the relative error roughly stays the same.

Figure 6 shows the results for Scenario D, where the number of clutter is uniformly distributed. This is different from the other scenarios because here, we estimate a Poisson rate for data that is not Poisson distributed. Therefore, it is not possible to quantify the error of the estimation. Instead, we only show the estimated clutter rate and our proposed QI. The estimated rate is roughly the same as the mean of the uniform distribution. This is not surprising, as the mean of a Poisson distribution is given by its rate. However, the QI of the estimation is large. Therefore, the QI correctly indicates that the quality of the estimation is low, especially compared to scenario A, where the number of clutter also follows a time-invariant distribution.

To summarize, the proposed clutter rate estimation with included self-monitoring correctly estimates the clutter rate in all scenarios. It follows jumps and drifts of the clutter rate, and the proposed QI value is an online value that indicates when the estimation is not reliable.

VII. Conclusion and Future Work

This work contributed to the *assessment of tracking parameters*. We presented a self-monitored clutter rate estimation for the LMB filter. The developed method provides an estimation of the clutter rate together with the QI, a value indicating the quality of the estimation. The significance of the QI was demonstrated by comparing it to the estimation error computed with ground truth data. This evaluation showed a high correlation between the two values, meaning that the online calculable QI can indicate phases where the estimation is not as reliable as before. Additionally, the QI can be used to

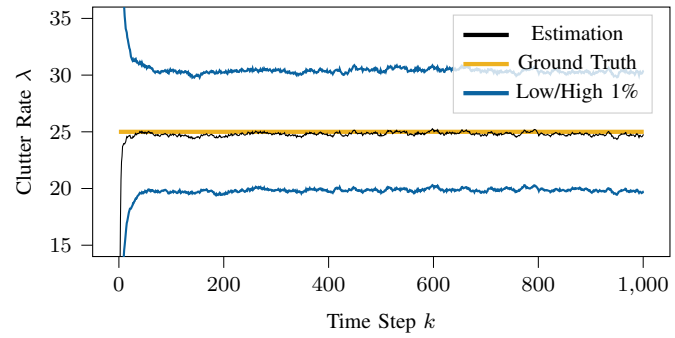

(a) Clutter rate estimation of scenario A.

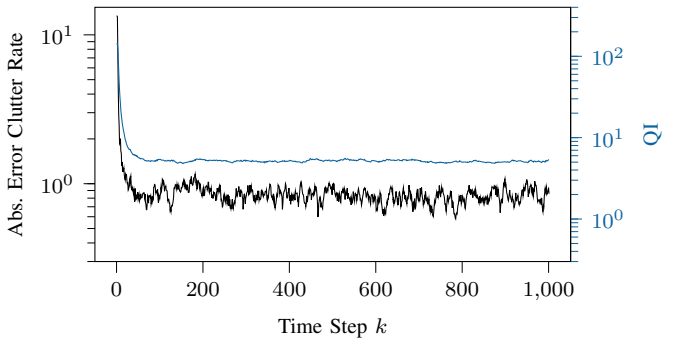

(b) Estimation error of scenario A compared to the proposed QI.

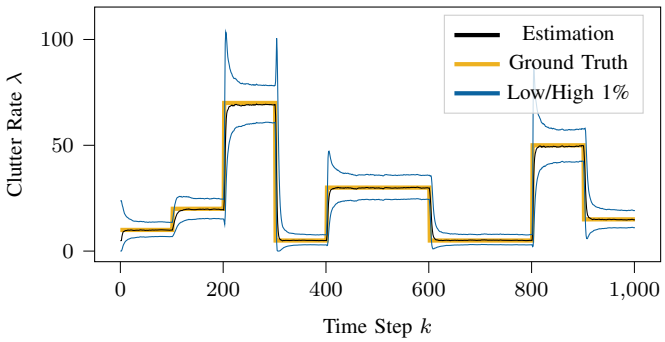

(c) Clutter rate estimation of scenario B.

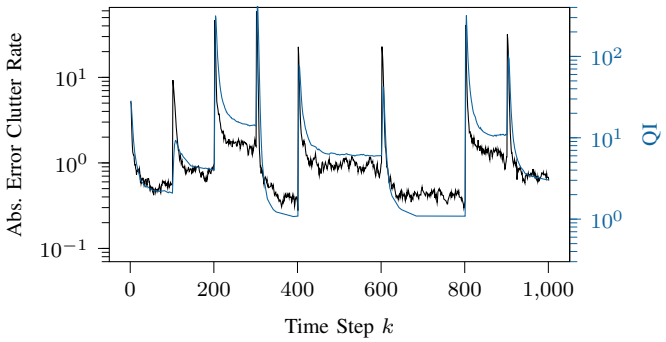

(d) Estimation error of scenario B compared to the proposed QI.

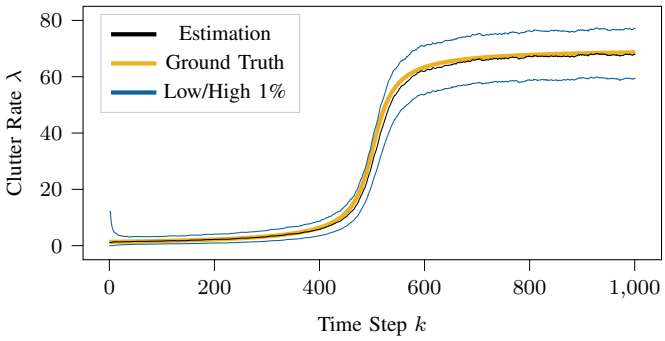

(e) Clutter rate estimation of scenario C.

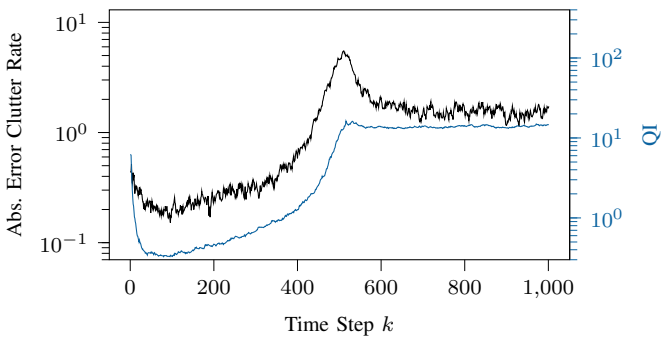

(f) Estimation error of scenario C compared to the proposed QI.

Fig. 5: Results for the three clutter scenarios A, B, and C from Fig. 1. The left column shows the current estimation in black together with the high and low 1% quantile of the estimated Gamma distribution. The real value of the clutter rate is shown by the thick yellow line. On the right, we show the estimation error together with the proposed QI. Note that the estimation error requires ground truth knowledge, whereas the QI does not.

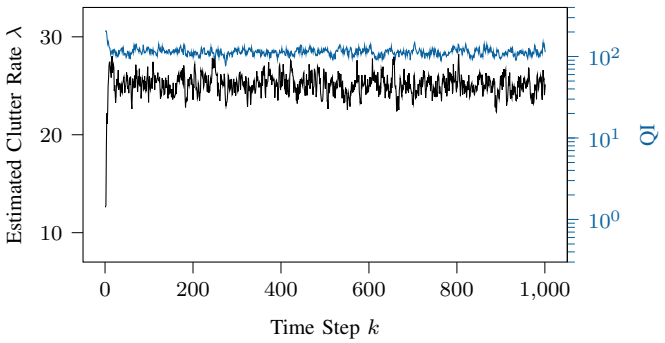

Fig. 6: Clutter rate estimation and proposed QI of scenario D, where the number of clutter is uniformly distributed.

detect situations where the number of clutter does not follow the expected distribution.

The results of this work will be used in future work that provides the *sensitivity of the tracking parameters*. Put together, this will allow an estimation of the impact of a parameter misconfiguration. In addition, methods for the quantitative evaluation of self-assessment need to be developed.

References

[1] M. Henning, J. Müller, F. Gies, M. Buchholz, and K. Dietmayer, "Situation-Aware Environment Perception Using a Multi-Layer Attention Map," *IEEE Transactions on Intelligent Vehicles*, vol. 8, no. 1, pp. 481–491, Jan. 2023.

[2] Bundesministerium der Justiz sowie das Bundesamts für Justiz. (2022) Verordnung zur Genehmigung und zum Betrieb von Kraftfahrzeugen mit

autonomer Fahrfunktion in festgelegten Betriebsbereichen (Autonome-Fahrzeuge-Genehmigungs-und Betriebs-Verordnung - AFGBV). [Online]. Available: https://www.gesetze-im-internet.de/afgbv/AFGBV.pdf

[3] D. Schuhmacher, B.-T. Vo, and B.-N. Vo, "A Consistent Metric for Performance Evaluation of Multi-Object Filters," *IEEE Transactions on Signal Processing*, vol. 56, no. 8, pp. 3447–3457, Aug. 2008.

[4] M. Beard, B. T. Vo, and B.-N. Vo, "OSPA $^{(2)}$: Using the OSPA metric to evaluate multi-target tracking performance," in *2017 International Conference on Control, Automation and Information Sciences (ICCAIS)*, Chiang Mai, Thailand, Oct. 2017, pp. 86–91.

[5] A. S. Rahmathullah, A. F. Garcia-Fernandez, and L. Svensson, "Generalized optimal sub-pattern assignment metric," in *2017 20th International Conference on Information Fusion (Fusion)*, Xi'an, China, Jul. 2017, pp. 1–8.

[6] J. Duník, O. Straka, and B. Noack, "Classification of Uncertainty Sources for Reliable Bayesian Estimation," in *2023 IEEE Symposium Sensor Data Fusion and International Conference on Multisensor Fusion and Integration (SDF-MFI)*, Bonn, Germany, Nov. 2023, pp. 1–8.

[7] S. Reuter, B.-T. Vo, B.-N. Vo, and K. Dietmayer, "The labeled multi-bernoulli filter," *IEEE Transactions on Signal Processing*, vol. 62, no. 12, pp. 3246–3260.

[8] Y. Bar-Shalom and T. Fortmann, *Tracking and Data Association*. Academic Press, 1988.

[9] R. Mahler, "Divergence detectors for multitarget tracking algorithms," I. Kadar, Ed., Baltimore, Maryland, USA, May 2013, p. 87450F.

[10] T. Griebel, J. Müller, M. Buchholz, and K. Dietmayer, "Kalman Filter Meets Subjective Logic: A Self-Assessing Kalman Filter Using Subjective Logic," in *2020 IEEE 23rd International Conference on Information Fusion (FUSION)*, Jul. 2020, pp. 1–8.

[11] T. Griebel, J. Müller, P. Geisler, C. Hermann, M. Herrmann, M. Buchholz, and K. Dietmayer, "Self-assessment for single-object tracking in clutter using subjective logic," in *2022 25th International Conference on Information Fusion (FUSION)*, 2022, pp. 1–8.

[12] A. Jøsang, *Subjective Logic*. Cham: Springer International Publishing, 2016.

[13] B.-T. Vo and B.-N. Vo, "Labeled Random Finite Sets and Multi-Object Conjugate Priors," *IEEE Transactions on Signal Processing*, vol. 61, no. 13, pp. 3460–3475, Jul. 2013, number: 13.

[14] A. Gelman, J. B. Carlin, H. S. Stern, D. B. Dunson, A. Vehtari, and D. B. Rubin, "Bayesian Data Analysis Third edition (with errors fixed as of 15 February 2021)."

[15] R. P. S. Mahler, *Statistical multisource-multitarget information fusion*. Boston: Artech House, 2007.

[16] M. Herrmann, C. Hermann, and M. Buchholz, "Distributed Implementation of the Centralized Generalized Labeled Multi-Bernoulli Filter," *IEEE Transactions on Signal Processing*, vol. 69, pp. 5159–5174, 2021.

[17] J. Strohbeck, J. Müller, A. Holzbock, and M. Buchholz, "Deepsil: A software-in-the-loop framework for evaluating motion planning schemes using multiple trajectory prediction networks," in *International Conference on Intelligent Robots and Systems*, 2021, pp. 7075–7081.